SAC: G: Planning and Coordination for Air-Ground Robots in Persistent Monitoring Applications with Visibility Constraints

Parikshit Maini
Dept. of CSE, IIIT-Delhi, India.
parikshitm@iiitd.ac.in

ABSTRACT

In this work we address a set of problems within the larger domain of "visual monitoring using autonomous robots". The first problem addresses the use of a ground-based mobile refueling vehicle to increase the operational range of a fuel constrained unmanned aerial vehicle (UAV) to perform large-scale visual monitoring. A solution method for the problem must account for fuel constraints of the aerial vehicle, terrain restrictions of the ground vehicle and speed differential of the two vehicles while ensuring area coverage. We develop branch-and-cut based exact and heuristic solution methods for this problem. The second problem, relates to visual monitoring on terrains using multiple heterogeneous robotic sensors. We develop mixed integer linear programming (MILP) based exact methods to perform long term persistent monitoring of piecewise linear features (path-like) within a terrain. A path-like feature on a terrain is modeled as an x-monotone curve to build an efficient represent for visibility structures. As extension to these results, in the third problem we address the multi-point monitoring problem on a polyhedral terrain using an aerial robot. The points-of-interest may be located anywhere within the terrain. The route planning problem is posed as an instance of TSP with neighborhoods (TSPN). We develop a constant-factor approximation algorithm for the given instance of TSPN. The problem is further reduced to an instance of generalized TSP (GTSP). A branch-and-cut method is used to solve the GTSP instance and compared against solutions computed using a state-of-the-art tool - GLNS. For each of the problems addressed, we also perform outdoor experimental validations on actual robots.

KEYWORDS

multi-robot systems, persistent planning, cooperative planning, visual monitoring, route planning

ACM Reference Format:
Parikshit Maini. 2019. SAC: G: Planning and Coordination for Air-Ground Robots in Persistent Monitoring Applications with Visibility Constraints. In *Proceedings of SAC'18 Applied Computing*. ACM, New York, NY, USA, 6 pages. https://doi.org/10.1145/nnnnnnn.nnnnnnn

SAC'18 Applied Computing, April 09–13, 2018, Pau, France

ACM ISBN 978-x-xxxx-xxxx-x/YY/MM…$15.00
https://doi.org/10.1145/nnnnnnn.nnnnnnn

Introduction

Visual Monitoring using autonomous robots is an important problem that occurs in applications like ISR (Intelligence, Surveillance and Reconnaissance)[6, 11, 12, 20], disaster management [21, 24] and structural monitoring [8, 22, 28]. The use of cooperative aerial and ground robot systems for monitoring tasks is an active area of research and has garnered a lot of interest from the research community over the last few years. In this work, we address a set of problems under the general theme of "visibility-based monitoring using robotic sensor nodes under various system and application constraints".

The first problem, Fuel Constrained UAV Routing Problem using a Mobile Refueling Station (FCURP-MRS), relates to large-scale visual coverage using a UAV (Figure 1a). In this context, large-scale implies missions involving geographically large areas and/or large temporal space (for example: persistent missions). A UAV cannot complete such a mission in a single flight and needs refueling to extend its operational range in both space and time. We propose the use of a mobile ground-based refueling station to refuel the UAV. The UAV must rendezvous with the refueling ground vehicle (GV) to refuel. Further, we restrict the GV to traverse on the road network available within the operational region to account for practical considerations. We were the first to solve the joint UAV-GV routing problem with refueling considerations [13, 16–18]. Existing works in the literature either used stationary refueling stations [10, 30] or considered fixed UAV routes to *schedule* recharging windows for the ground vehicles[23]. In recent times, the problem has been addressed by many research teams and different solution methods have been developed [2, 29, 33]. We have designed a two stage framework to solve FCURP-MRS. The first stage computes refueling sites on the road network while accounting for terrain restrictions of the GV and fuel limitations of the UAV. The second stage solves the joint UAV-GV route planning problem while respecting refueling constraints of the UAV and speed differential of the two vehicles. Our two-stage framework has also been used by others working on this problem [29]. We develop MILP formulations for the coupled routing problem. We also develop a greedy solution and a construction heuristic based on solving a TSP sub-instance.

The second problem, Heterogeneous Watchmen Persistent Routing Problem on a Terrain (HWPRPT), extends the visual coverage solution to terrains (Figure 1b). A terraineous environment adds visibility constraints to the problem. We address a special case of monitoring a path-like feature (piece-wise linear) within a terrain. We develop methods on the use of multiple aerial and ground robotic sensor nodes to perform a persistent coverage mission. The problem is a generalization of n - Watchman Routing Problem (n-WRP) to the heterogeneous robotic sensor case. [3] show

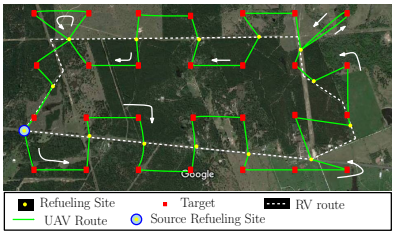

(a) FCURP-MRS instance

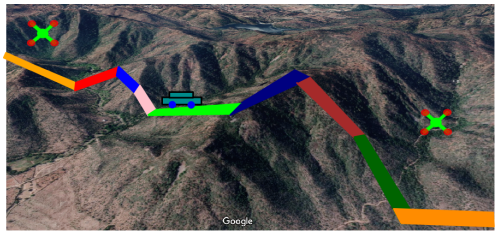

(b) HWPRPT instance

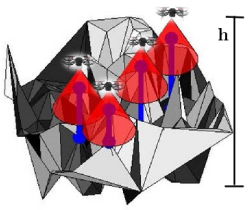

(c) URPT instance

that n-WRP for homogeneous watchmen is NP-hard. Due to inherent complexity of the problem, practical solution approaches including decoupled viewpoint selection and robot routing [27] and self-organizing map heuristics [7] have been proposed in the literature. There have also been efforts to design algorithms for restricted polygon domains: spiral polygons [26], histograms [4], and more recently street polygons[3, 31]. All of these approaches address the homogeneous robot (watchman) case. Our work addresses the heterogeneous watchmen scenario for persistent monitoring application [14, 19]. This also involves refueling the UAVs and placement of stationary refueling stations within the terrain. We optimize over a challenging objective function that considers both robot cost balancing and refueling station placement. We model the path-like feature as a x-monotone curve and develop an efficient discrete characterization of visibility regions that cover each point on the terrain. We address multiple sub-problems in this domain to build a solution to the eventual persistent monitoring problem. Our solution methods comprise of a MILP based branch-and-cut method and a construction heuristic based on solving a TSP sub-instance.

The third problem addressed in this work, UAV Routing Problem on Terrains (URPT), solves the multiple-point visual monitoring problem on a terrain using a UAV with a limited field-of-view (Figure 1c). A solution to the problem comprises of a route for the UAV that covers each point-of-interest on the terrain while accounting for visibility restrictions due to the terrain and limited field-of-view of the UAV. Area decomposition based on camera footprint and/or obstacle-free space is a popular solution approach in the literature and admits a robust discretization of the area of interest [1, 5, 9, 25, 32]. Other techniques include seed-spreader algorithms [32], potential fields [9] and graph-based search algorithms [25]. However, most of the existing works on coverage path-planning assume a flat surface and do not account for altitude variance (and hence the visibility obstructions) of the ground surface. A closely related work is that of Choi et. al. [5], who address a constant resolution coverage problem that takes into account camera viewing direction and altitude to maintain the image resolution. In this work, we address a multiple-point monitoring problem using an aerial robot while explicitly accounting for visibility restrictions due to the shape of the terrain and camera field of view. We extend our terrain model to a 2.5 D representation. Our solution approach involves computing visibility regions for each point-of-interest. We reduce the problem to an instance of TSPN and design a constant-factor approximation algorithm for the TSPN instance. We further reduce the problem to GTSP and develop an Integer Linear Program (ILP) to compute routes for the UAV [15].

For each problem addressed in this work extensive computational simulations and outdoor experimental validations were performed.

1 ROBOT MODEL

The aerial robot model used in this work is a multi-rotor type vertical take-off and landing (VTOL) model. It operates at a constant altitude and constant air speed. Each individual robot has a given maximum fuel capacity, U. Assuming a constant rate of fuel consumption, regardless the maneuver, and a constant speed for each robot; flight time, distance traveled, fuel consumed and cost are proportional quantities and are used interchangeably. Further, the operating cost of aerial robots is directly proportional to Euclidean distance traversed and flight altitude. We assume ideal flying conditions and do not consider the effects of wind.

The ground robot is assumed to have infinite fuel availability and does not run out of fuel. The operating cost of a ground robot is asymmetric on terrains. It incur a larger cost for uphill traversals and a lower cost for downhill traversals. Further, robots do not have communication capabilities.

Specific to FCURP-MRS: GV travels at a constant speed and R is the maximum distance traveled it can travel in a single flight time of the UAV. The UAV may only land on the GV. It may hover at the refueling site if the GV has not reached, but the total fuel consumed by the UAV must not exceed U.

2 FCURP-MRS

Consider an environment ($\mathcal{E}$) with an interior road network (Fig. 1a), a UAV with a fixed down-facing camera on board and a refueling ground vehicle (GV) that traverses on the given road network. To perform a coverage mission, place data points or *targets* (T) in $\mathcal{E}$ in a manner that the camera footprint of T exhaustively covers the environment $\mathcal{E}$. The UAV must capture imagery of the environment from each of the targets in $\mathcal{T}$ to complete a visual survey of the area. It cannot visit all targets in a single flight. This necessitates refueling, possibly multiple times, to complete the mission. The UAV must rendezvous with the GV to refuel. The rendezvous locations are referred to as *refueling sites* (S).

Refueling Site Selection

The refueling site selection algorithm computes a set of candidate refueling sites, $\mathcal{S}$, by uniformly sampling the road network. For a set $S \subseteq \mathcal{S}$, to be deemed as a valid set of refueling sites, it must satisfy the following two conditions:

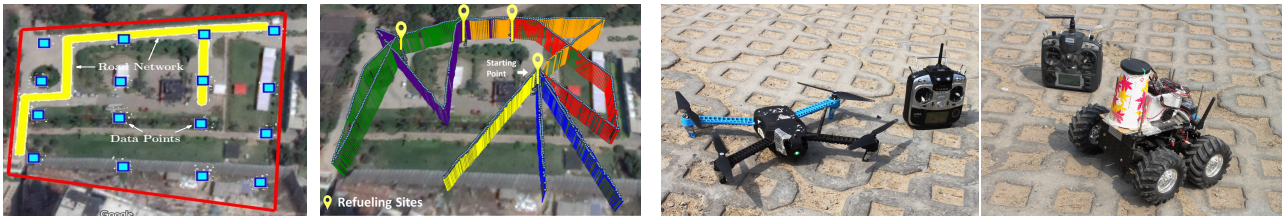

(a) (b) (c) (d)

Figure 2: FCURP-MRS experiment results: (a) Environment setup (b) Sample output paths computed using the edge-based formulation as traversed by the UAV. (c) UAV: 3DR IRIS+, used in the experiments. (d) Ground Vehicle used.

(1) **Coverage condition:** There exists a refueling site $s \in S$, for each target $t \in T$, such that the distance between s and t is at most $U/2$ units.
(2) **Connectedness condition:** Refueling sites in S form a connected component in the graph G_r, where $G_r \equiv (S, E)$; an edge (i, j) where $i, j \in S$ is contained in the set E if and only if the distance between i and j via the road network (road distance) is at most R units.

A greedy algorithm based on computing distance constrained hitting sets, where discs of radii $U/2$ centered at the data points within T form sets and $\mathcal{S}$ represents the set of elements, is used to compute a valid set of refueling sites. The set ensures that there exists a feasible solution to the joint routing problem of a UAV and RV in the presence of refueling constraints for the UAV.

Mathematical formulation

The minimal set of refueling sites, S, obtained from the refueling site selection algorithm is an input to the UAV-GV joint routing problem. UAV and GV are initially stationed at a common refueling site, $s_0 \in S$, and return to the same location after the mission. MILP formulations are developed using two different paradigms to solve the joint route planning problem with fuel constraints: edge-based and node-based. The FCURP-MRS is formulated on a complete directed graph $G = (V, E)$, with vertex set $V = T \bigcup S$ and edge set E. Associated with the edge set are two weight functions: $f : E \rightarrow \mathbb{R}^+$, where f_{ij} denotes the fuel consumed by UAV when it travels along the directed edge (i, j) and $r : (S \times S) \rightarrow \mathbb{R}^+$, that represents the road distance between two refueling sites. Let $N : S \rightarrow \wp(S)$, where $\wp(S)$ is the power set of S, denote a neighborhood function defined as $N(s_i) := \{s_j : r_{ij} \leq R, s_j \in S\}$. For any subset of vertices $P \subseteq V$, we define $\delta^+(P) := \{(i, j) : (i, j) \in E, i \in P, j \notin P\}$. Further, $M = U + \max_{(i,j)} f_{ij}$, represents a large constant.

$$\mathcal{F}_1 : \text{ minimize} \sum_{i \in V} \sum_{j \in V} f_{ij} x_{ij}. \tag{1}$$

Degree constraints:

$$\sum_{i \in V \setminus \{j\}} x_{ij} = \sum_{i \in V \setminus \{j\}} x_{ji}, \quad \forall j \in V \text{ and} \tag{2}$$

$$\sum_{i \in V \setminus \{t\}} x_{it} = 1, \quad \forall t \in T. \tag{3}$$

$$\sum_{(i,j) \in \delta^+(P)} x_{ij} \geq 1, \quad \forall P \subseteq V \setminus \{s_0\}, P \cap T \neq \phi. \tag{4}$$

Fuel constraints:

$$u_t - u_j + f_{jt} \leq M(1 - x_{jt}), \quad \forall t, j \in T, \tag{5}$$

$$u_t - u_j + f_{jt} \geq -M(1 - x_{jt}), \quad \forall t, j \in T, \tag{6}$$

$$u_t - U + f_{kt} \leq M(1 - x_{kt}), \quad \forall t \in T, \forall k \in S, \tag{7}$$

$$u_t - U + f_{kt} \geq -M(1 - x_{kt}), \quad \forall t \in T, \forall k \in S, \tag{8}$$

$$-u_t + f_{tk} \leq M(1 - x_{tk}), \quad \forall t \in T, \forall k \in S, \tag{9}$$

$$f_{ij} \cdot x_{ij} \leq U \quad \forall i, j \in S, \tag{10}$$

$$\sum_{i \in V} \sum_{j \in V} f_{ij} x_{ij} \leq U \sum_{k \in S} \sum_{i \in V} x_{ki}. \tag{11}$$

Refueling site constraints:

$$y_{ts} - x_{st} \geq 0, \quad \forall t \in T, s \in S, \tag{12}$$

$$y_{t_2 s} - y_{t_1 s} \leq (1 - x_{t_1 t_2}), \quad \forall s \in S, \forall t_1, t_2 \in T, \tag{13}$$

$$y_{t_2 s} - y_{t_1 s} \geq -(1 - x_{t_1 t_2}), \quad \forall s \in S, \forall t_1, t_2 \in T, \tag{14}$$

$$\sum_{k \in S \setminus N(s)} x_{tk} \leq (1 - y_{ts}), \quad \forall t \in T, s \in S, \tag{15}$$

$$\sum_{k \in S \setminus N(s)} x_{sk} = 0, \quad \forall s \in S, \tag{16}$$

$$\sum_{s \in S} y_{ts} = 1, \quad \forall t \in T. \tag{17}$$

Variable restrictions:

$$x_{ij} \in \{0, 1\}, \quad \forall (i, j) \in E, \text{either } i \text{ or } j \in T \tag{18}$$

$$u_i \in [0, U], \quad \forall i \in T, \tag{19}$$

$$y_{ts} \in \{0, 1\}, \quad \forall t \in T, s \in S. \tag{20}$$

The MILP formulation is implemented within a branch-and-cut framework owing to the exponential size of constraint set (4).

Ground Vehicle Route

The MILP formulation ensures in any feasible solution that consecutive visits to refueling sites on the UAV tour are within R road distance. The tour comprising refueling site visits in the sequence as they occur on the UAV tour is a valid tour for the GV and ensures feasibility of the UAV tour. The tour so computed, ensures that the GV, when traveling at the constant speed V_r, always reaches the refueling site before the UAV runs out of fuel.

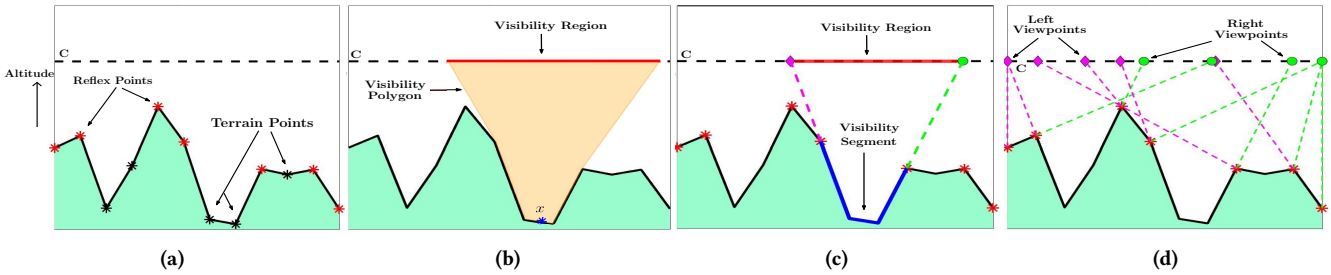

Figure 3: (a) Terrain points, reflex points and a fixed altitude path, C, chain visible with the terrain. (b) Visibility polygon and visibility region corresponding to a point x on the terrain. (c) A visibility segment and its corresponding visibility region. (d) Left and right viewpoints for all visibility segments.

Computational simulations comparing the various solution approaches - greedy, TSP-based heuristic and MILP formulations were performed to benchmark solution quality. Field experiments using actual robots were performed to test performace. Figure 2a show the environment used in the experiment along with road-network. Sample solution path generated using MILP formulation as traversed by the UAV are shown in Figure 2b.

3 HWPRPT

To compute a feasible solution for HWPRPT, we model the environmental feature to be monitored as a 1.5 Dimensional structure ($x-monotone$ curve). A 1.5 D model is characterized by *terrain points* and *reflex points* (Figure 3a). A terrain point is any point on the surface of the terrain that observes a change in slope. The set of reflex points is a subset of the set of terrain points. A reflex point is a terrain point which observes a decrease in slope when visited in the left to right direction.

Chain Visibility

A curve C and a set of points X in 2 D are said to be *chain visible* if for each point $x \in X$, the intersection of the visibility polygon, i.e. space that has an unrestricted view of x (Figure 3b), and C is either an empty set or a connected chain [31]. We refer to this intersection region as the *visibility region* for the point x on the curve C. In the case of HWPRPT, the fixed altitude paths correspond to aerial robot flight altitudes and the set of points X comprises points that lie on the terrain. Also, a curve is chain visible to any set of points that lie on the curve itself, hence the terrain (ground robot path) itself is a chain visible curve for points on the terrain.

Visibility Segments, Regions and Viewpoints

The surface of a 1.5 D terrain between two consecutive reflex points forms a convex polyline, when observed from a point on the terrain or on the constant-altitude flight path, and is called a *visibility segment* (or a segment) (Figure 3c). The region on the constant-altitude flight path between extended projections of the right edge of the left reflex point and left edge of the right reflex point of the visibility segment, is referred to as the *visibility region* of the given visibility segment[1]. Visibility region of a segment is a continuous curve and represents the intersection of visibility region for each point within the segment. Its continuity is attributed to the property of chain visibility between the pair of robot (flight) paths and the 1.5D terrain, and convexity of the visibility segment. Left and right end-points of a visibility region are referred to as the left and right viewpoints, respectively, of the corresponding visibility segment (Figure 3d).

[1]In case of visibility obstructions, the projections are suitably adjusted to pass through the obstructing reflex point to compute the visibility region.

Solution Approach

We develop a MILP formulation solved within a branch-and-cut framework to compute exact solutions to the problem. The discrete optimization model could only be developed by virtue of visibility priors discussed above, that restrict the search space to segment viewpoints on the chain visible curves corresponding to each robot. The formulation optimizes over a min-max objective function that balances load over all robots available. It also account for placement of refueling stations within the environment. We also conduct extensive computation simulations (Figures 4a and 4b). As expected the computation time increases exponentially with increase in instance size.

We also perform outdoor experiments to validate the strategy. The experiments were performed using four robots: two aerial and two ground. To perform the experiments a simulated piece-wise linear feature was used superimposed with a simulated 1.5 D terrain. The MILP solver was used to generate routes for each robot. The validation experiments were successfully abel to show coverage for the entire feature by traversing the routes generated by the solver.

4 URPT

In this problem we develop routes for a UAV to cover a set of points-of-interest. The points lie on a terrain that adds visibility constraints. We represent the topographical surface within the environment using a polyhedral (or 2.5 D) terrain and model it as a triangular irregular network (TIN). The UAV is assumed to have a fixed down-facing camera with a limited field-of-view. We consider a circular field-of-view for ease of exposition. To compute a feasible solution to the problem each point-of-interest must be covered on the UAV path. To ensure the same, we compute visibility regions on the constant altitude flight plane (Figure 5a) using the global horizons. For each point-of-interest we compute its global horizon (line). The global horizon gives the elevation of the farthest point in each radial direction. For each radial direction, we compute the complement of

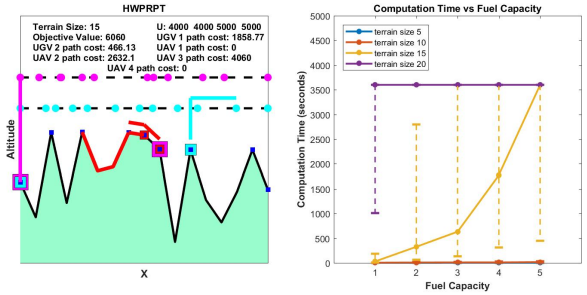

(a) (b)

Figure 4: HWPRPT Simulation Results: (a) Routes generated by the solver for a sample environment. The paths are color coded. Red color represents ground robots, cyan color represents robots flying at altitude 1 and magenta color represents aerial robots flying at altitude 2. (b) Computation time vs fuel capacity plot for MILP solver.

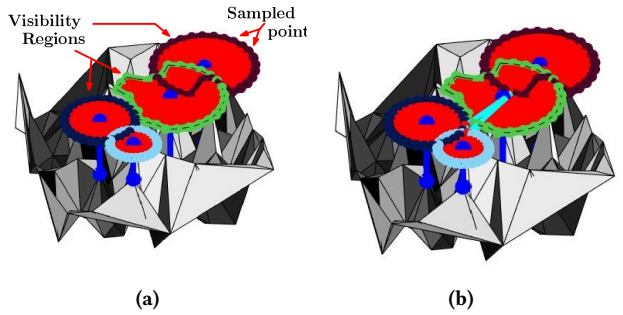

(a) (b)

Figure 5: URPT Simulation Results: (a) Visibility regions for points-of-interest (b) Sample solution generated using ILP solver. The tour is shown in cyan color.

the elevation of the horizon. In each radial direction, the minimum of camera field-of-view angle and the complement computed, is used as the visibility angle. The locii of radial visibility angles for each point-of-interest when projected on to the constant altitude flight plane, return the visibility region for each point. The regions so computed may not have a regular geometrical shape.

To compute a solution to URPT, we need to find a tour that visit each of the visibility regions. This is an instance of the TSP with Neighborhoods problem. We develop a constant-factor approximation for this category of neighborhoods. Further, using existing results in the literature that remark that any optimal solution would visit each region only on the boundary, we restrict our search. By doing a uniform sampling on the boundary we are able to reduce the problem to an instance of GTSP (Figure 5b). We solve the GTSP instance using a ILP formulation implemented in a branch-and-cut framework and compare against solutions computed by a standard GTSP tool. We also perform field experiments to test our approach. Figures 6a and 6b show the experiment environment and UAV path computed.

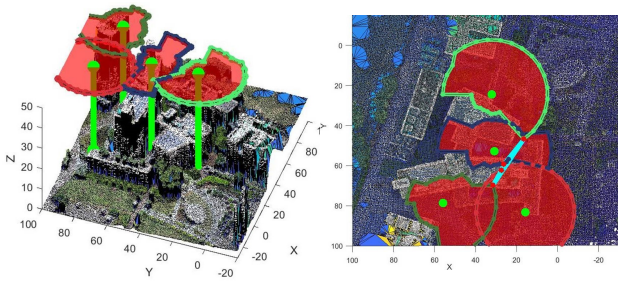

(a) (b)

Figure 6: URPT experiment results: (a) Visibility regions for the monitoring targets. (b) Top view of the operational area showing the UAV path in cyan color.

REFERENCES

[1] J. F. Araújo, P. B. Sujit, and J. B. Sousa. 2013. Multiple UAV area decomposition and coverage. In *Symposium on Computational Intelligence for Security and Defense Applications*. 30–37.

[2] Barbara Arbanas, Antun Ivanovic, Marko Car, Matko Orsag, Tamara Petrovic, and Stjepan Bogdan. 2018. Decentralized planning and control for UAV–UGV cooperative teams. *Autonomous Robots* 42, 8 (2018), 1601–1618.

[3] S. Carlsson, H. Jonsson, and B. J. Nilsson. 1999. Finding the Shortest Watchman Route in a Simple Polygon. *Discrete & Computational Geometry* 22, 3 (01 Oct 1999), 377–402.

[4] Svante Carlsson, Bengt J Nilsson, and Simeon Ntafos. 1991. Optimum guard covers and m-watchmen routes for restricted polygons. In *Workshop on Algorithms and Data Structures*. Springer, 367–378.

[5] Y. Choi, Y. Choi, S. Briceno, and D. N. Mavris. 2018. Three-dimensional UAS Trajectory Optimization for Remote Sensing in an Irregular Terrain Environment. In *International Conference on Unmanned Aircraft Systems*. 1101–1108. https://doi.org/10.1109/ICUAS.2018.8453310

[6] Wendell H Chun and Nikolaos Papanikolopoulos. 2016. Robot surveillance and security. In *Springer Handbook of Robotics*. Springer, 1605–1626.

[7] J. Faigl. 2010. Approximate Solution of the Multiple Watchman Routes Problem With Restricted Visibility Range. *IEEE Transactions on Neural Networks* 21, 10 (Oct 2010), 1668–1679. https://doi.org/10.1109/TNN.2010.2070518

[8] Youngjib Ham, Kevin K. Han, Jacob J. Lin, and Mani Golparvar-Fard. 2016. Visual monitoring of civil infrastructure systems via camera-equipped Unmanned Aerial Vehicles (UAVs): a review of related works. *Visualization in Engineering* 4, 1 (06 Jan 2016), 1. https://doi.org/10.1186/s40327-015-0029-z

[9] Ibrahim A Hameed, Anders la Cour-Harbo, and Ottar L Osen. 2016. Side-to-side 3D coverage path planning approach for agricultural robots to minimize skip/overlap areas between swaths. *Robotics and Autonomous Systems* 76 (2016), 36–45.

[10] Tanya E Kannon, Sarah G Nurre, Brian J Lunday, and Raymond R Hill. 2014. The aircraft routing problem with refueling. *Optimization Letters* (2014), 1–16.

[11] Thomas Kopfstedt, Masakazu Mukai, Masayuki Fujita, and Christoph Ament. 2008. Control of formations of UAVs for surveillance and reconnaissance missions. *IFAC Proceedings Volumes* 41, 2 (2008), 5161–5166.

[12] Heba Kurdi, Jonathon How, and Guillermo Bautista. 2016. Bio-inspired algorithm for task allocation in multi-UAV search and rescue missions. In *AIAA Guidance, Navigation, and Control Conference*. 1377.

[13] Parikshit Maini. 2018. Cooperative Routing with Refueling for Aerial and Ground Vehicles for Large Scale Surveillance: Student Research Abstract. In *Proceedings of the 33rd Annual ACM Symposium on Applied Computing (SAC '18)*. ACM, New York, NY, USA, 847–848. https://doi.org/10.1145/3167132.3167450

[14] Parikshit Maini, Gautam Gupta, Pratap Totekar, and Sujit P. B. 2018. Visibility-based monitoring of a path using a heterogeneous robot team. In *IEEE/RSJ International Conference on Intelligent Robots and Systems*.

[15] Parikshit Maini, P. B. Suijt, and Pratap Tokekar. 2019. Visual Monitoring for Multiple Points of Interest on a 2.5D Terrain using a UAV with Limited Field-of-View Constraint. *CoRR* abs/1903.07363 (2019). arXiv:1903.07363 http://arxiv.org/abs/1903.07363

[16] P. Maini and P.B. Sujit. 2015. On cooperation between a fuel constrained UAV and a refueling UGV for large scale mapping applications. In *International Conference on Unmanned Aircraft Systems*. 1370–1377.

[17] Parikshit Maini, Kaarthik Sundar, Sivakumar Rathinam, and P. B. Sujit. 2018. Cooperative Planning for Fuel-constrained Aerial Vehicles and Ground-based

Refueling Vehicles for Large-Scale Coverage. *CoRR* abs/1805.04417 (2018). arXiv:1805.04417 http://arxiv.org/abs/1805.04417

[18] Parikshit Maini, Kaarthik Sundar, Madeep Singh, Sivakumar Rathinam, and P. B. Sujit. 2019. Cooperative aerial-ground vehicle route planning with fuel constraints for coverage applications. *IEEE Trans. Aerospace Electron. Systems* (2019).

[19] Parikshit Maini, Kevin Yu, PB Sujit, and Pratap Tokekar. 2018. Persistent monitoring with refueling on a terrain using a team of aerial and ground robots. In *2018 IEEE/RSJ International Conference on Intelligent Robots and Systems (IROS)*. IEEE, 8493–8498.

[20] Satyanarayana G Manyam, Steven Rasmussen, David W Casbeer, Krishnamoorthy Kalyanam, and Suresh Manickam. 2017. Multi-UAV routing for persistent intelligence surveillance & reconnaissance missions. In *Unmanned Aircraft Systems (ICUAS), 2017 International Conference on*. IEEE, 573–580.

[21] Lorenzo Marconi, Claudio Melchiorri, Michael Beetz, Dejan Pangercic, Roland Siegwart, Stefan Leutenegger, Raffaella Carloni, Stefano Stramigioli, Herman Bruyninckx, Patrick Doherty, et al. 2012. The SHERPA project: Smart collaboration between humans and ground-aerial robots for improving rescuing activities in alpine environments. In *Safety, Security, and Rescue Robotics (SSRR), 2012 IEEE International Symposium on*. IEEE, 1–4.

[22] Koppány Máthé and Lucian Buşoniu. 2015. Vision and control for UAVs: A survey of general methods and of inexpensive platforms for infrastructure inspection. *Sensors* 15, 7 (2015), 14887–14916.

[23] Neil Mathew, Stephen L Smith, and Steven L Waslander. 2015. Planning paths for package delivery in heterogeneous multirobot teams. *IEEE Transactions on Automation Science and Engineering* 12, 4 (2015), 1298–1308.

[24] Robin R Murphy. 2014. *Disaster robotics*. MIT press.

[25] LH Nam, L Huang, XJ Li, and JF Xu. 2016. An approach for coverage path planning for UAVs. In *IEEE international workshop on advanced motion control (AMC)*. IEEE, 411–416.

[26] B. J. Nilsson and D. Wood. 1990. Optimum watchmen routes in spiral polygons. In *Canadian Conference on Computational Geometry*. 269–272.

[27] Eli Packer. 2008. Computing Multiple Watchman Routes. *Experimental Algorithms* (2008), 114–128.

[28] Sivakumar Rathinam, Zu Whan Kim, and Raja Sengupta. 2008. Vision-based monitoring of locally linear structures using an unmanned aerial vehicle. *Journal of Infrastructure Systems* 14, 1 (2008), 52–63.

[29] Fernando Ropero, Pablo Muñoz, and María D R-Moreno. 2019. TERRA: A path planning algorithm for cooperative UGV–UAV exploration. *Engineering Applications of Artificial Intelligence* 78 (2019), 260–272.

[30] Kaarthik Sundar and Sivakumar Rathinam. 2014. Algorithms for routing an unmanned aerial vehicle in the presence of refueling depots. *IEEE Transactions on Automation Science and Engineering* 11, 1 (2014), 287–294.

[31] Pratap Tokekar and Vijay Kumar. 2015. Visibility-based persistent monitoring with robot teams. In *IEEE/RSJ International Conference on Intelligent Robots and Systems*. 3387–3394.

[32] Anqi Xu, Chatavut Viriyasuthee, and Ioannis Rekleitis. 2011. Optimal complete terrain coverage using an unmanned aerial vehicle. In *International Conference on Robotics and Automation*. 2513–2519.

[33] Kevin Yu, Ashish Kumar Budhiraja, Spencer Buebel, and Pratap Tokekar. 2018. Algorithms and experiments on routing of unmanned aerial vehicles with mobile recharging stations. *Journal of Field Robotics* (2018).